

SEISMIC PERFORMANCE EVALUATION OF RC FRAMES IN RAILROAD VIADUCTS  
USING THREE-DIMENSIONAL NONLINEAR DYNAMIC ANALYSIS

(Translation from Proceedings of JSCE, No.662/V-49, November 2000)



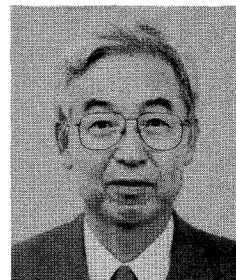
Satoshi TSUCHIYA



Yoshinobu FURUYA



Ick-Hyun KIM



Hajime OKAMURA

Focusing on the influence of multi-directional ground motion and of variations in material strength, the seismic performance of RC frames in railroad viaducts is evaluated using three-dimensional nonlinear dynamic analysis. The basis of analysis is a fiber technique. It is demonstrated that, in order to properly estimate seismic behavior, it is essential to use a three-dimensional analysis method that explicitly takes into account the effects of multi-directional motion. It is also reconfirmed that careful attention must be paid to material strength, and particularly the yield strength of the steel reinforcement. This method of analysis is an efficient and practical application of the latest technical understanding, and by combining the method with engineering judgment, seismic damage analysis becomes possible.

*Keywords: RC framed structures, seismic performance evaluation, 3D nonlinear dynamic frame analysis*

---

Satoshi Tsuchiya is a manager of COMS Engineering Corporation and a researcher in the Department of Civil Engineering at the University of Tokyo, Japan. He obtained his D.Eng. from the University of Tokyo in 2001. His research interests cover the seismic behavior and numerical analysis of reinforced concrete structures.

---

Yoshinobu Furuya is an engineer of Obayashi Corporation. He obtained his Master Degree from the University of Tokyo in 2001. His research interests relate to the seismic behavior of reinforced concrete structures and numerical analysis of underground cavern.

---

Kim, Ick-Hyun is a professor in the Civil and Environment Engineering at University of Ulsan, Korea. He obtained his Ph.D. from the University of Tokyo in 1998. His research interests cover the seismic behavior and numerical analysis of reinforced concrete structures. He is involved in the projects for the development of seismic design concept and seismic assessment in the moderate seismicity zone.

---

Hajime Okamura is the president of the Kochi University of Technology, Japan. He earned his D.Eng. from the University of Tokyo in 1966. The quantitative evaluation of reinforced concrete and the construction of high quality infrastructures with moderate cost have been investigated as his academic major backgrounds. He was the 87th president of Japan Society of Civil Engineers.

## 1. INTRODUCTION

Many reinforced concrete frames forming railroad viaducts suffered severe damage in the Hyogo-ken-Nanbu Earthquake of 1995 (also known as the Great Hanshin-Awaji Earthquake). In particular, shear failure caused heavy damage, including the complete collapse of RC piers [1]. The main reason for such failures may be taken to be an overestimation of the shear capacity of the concrete; this was typical of design at the time these bridges were constructed [2]. However, it is necessary to prevent similar failures in the future, and to support the development of procedures for seismic performance evaluation. The responsibility of concrete engineers is to provide rational explanations for phenomena affecting all bridges: how is ground motion propagated; how do structures respond; and what is the damage that results.

Previous investigations have shown that whether an RC pier bridge is damaged in shear or not can be macroscopically explained by introducing a key factor that is the ratio of shear capacity to flexural capacity of the piers [3][4]. Other bridges, however, remain a problem awaiting solution at present.

Kim et al. proposed a two-stage seismic performance evaluation method for RC frames in railroad viaducts [5][16] (Fig. 1). The first stage entails predicting failure modes by adopting the shear-flexural capacity ratio of the structure ( $V_u \cdot a / M_u$ ) as a ductility factor. If the shear capacity exceeds the flexural capacity ( $V_u \cdot a / M_u > 1.0$ ), the structure fails in flexure before shear failure. In this evaluation method, a safety factor is provided for the capacity ratio. If the ductility factor is larger than 1.3, the structure has adequate seismic performance (including ductility), whereas if it is smaller than 0.9, the structure is judged to have insufficient seismic performance. These criteria are determined in consideration of uncertainties, such as distributions in material strength. In the case of  $0.9 < V_u \cdot a / M_u < 1.3$ , where seismic performance cannot be evaluated very accurately at this first stage, a detailed evaluation that makes full use of the latest technology is carried out. This is the second stage of the evaluation. The methodology has progressed to a level where it is now practical to check the safety of a structure during an earthquake using three-dimensional nonlinear dynamic analysis with frame elements.

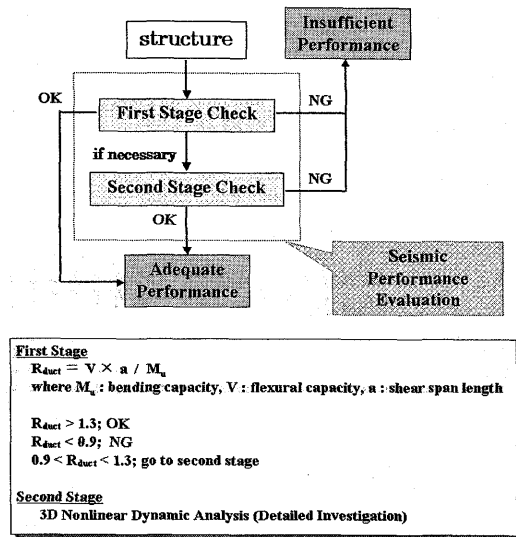


Fig.1 Seismic Performance Evaluation Method in Two Stages [5][16]

The great advantage of this evaluation method is that seismic performance can be judged more efficiently than by methods proposed and put into practical use by other research institutes. By isolating the majority of structures that do not require detailed analysis at the first stage, a great deal of labor can be saved. Consequently, this method is particularly suitable for infrastructure systems that include many target structures. However, detailed second-stage seismic evaluation analysis has so far not been carried out very widely, so comparative study of analytical results and actual damage remains as a subject of future study.

In investigating the seismic performance of RC frames in railroad viaducts, it is important to note that there are presently three types of uncertainty at the engineering level: the ground motion, the material properties, and the limitations of analysis tools. Therefore, it is necessary not only to investigate the failure mechanism as it is affected by each of these (by comparing actual damage with analytical results), but also to carry out an overall analysis by a macro method.

Seismic damage estimations by three-dimensional nonlinear dynamic analysis for multiple structures may enhance engineering knowledge in the following areas:

- 1) Clarifying factors that affect the seismic performance of structures
- 2) Moving toward a prediction method for ground motion at any location
- 3) Improving the reliability of structural analysis tools

On this occasion, it would be important to select not only damaged structures in shear and/or flexure but also

non-damaged ones.

This paper suggests need for, and validity of, three-dimensional nonlinear analysis prior to macro analysis for all RC frames in railroad viaducts, taking into consideration the two-stage seismic performance evaluation method proposed by Kim et al.

## **2. SEISMIC PERFORMANCE EVALUATION BY 3D NONLINEAR DYNAMIC ANALYSIS**

### **2.1 Summary of Analytical Method [6][15]**

An accurate analysis tool is necessary to carry out accurate examinations of the seismic performance of structures. In this study, the three-dimensional nonlinear dynamic analysis program *COM3\_Fiber*, developed by the concrete laboratory of the University of Tokyo [15] is used. It has been verified through comparative investigations with a shaking table that the nonlinear response behavior of a single RC pier under eccentric axial forces can be closely estimated with this program [7]. As regards the multi-directional behavior of Rahmen structures, although such a comparative verification against experiments has yet to be carried out, it may be assumed that accuracy will not decline significantly. This unverified assumption can be treated as part of the aforementioned uncertainty in the accuracy of the analysis tool.

The program *COM3\_Fiber* is a three-dimensional analysis tool with degenerate degrees of freedom. Frame elements are introduced to represent the reinforced concrete and elasto-plastic materials, with three-dimensional solid elements representing elasto-plastic materials. Interface elements are also introduced as necessary between frame elements to take into account local deformations such as pull-out of reinforcing bars. In principle, a three-dimensional analysis using RC solid elements should be applied to the detailed second-stage seismic evaluation to directly estimate failure and deformation. However, such an approach to dynamic response analysis is impractical at the moment although the full three-dimensional analysis tool including shear deformation has been already established. This is because criteria for judging failure during full three-dimensional analysis have not yet been well established, and a great deal of computational effort would be required. In this respect, progress from both hardware and software perspectives is expected, such as in the form of highly efficient computers and algorithms or by introducing multi-threaded processing. For that reason, three-dimensional analysis using frame elements based on fiber technique for RC piers is selected even in this study focusing on shear failure mainly.

The program *COM3\_Fiber* makes use of Timoshenko beam theory, which allows for shear deformation, and a very large shear stiffness is assumed. The shear failure criterion is given in the next section. The top slabs of the railroad viaducts are assumed to be elastic to simplify the computation. The reason for this is that damage to this part of the structure during an earthquake is minor aside from the possibility of falling from the piers because so much reinforcement is provided.

In the fiber technique, the sectional axial forces and moments in the two directions are calculated from the average axial strain and curvature in the two directions. In doing this, it is assumed that a plane section remains plane and that strain is distributed in a straight line at the section. With the application of suitable material constitutive models for concrete and reinforcing bars, this analytical tool is able to accurately represent the dynamic response of RC structures [7][15]. Since the method reduces the number of degrees of freedom, computations are stable and converge well. Further, the method uses path-dependent nonlinear constitutive models, including unloading and reloading loops for concrete and reinforcing bars, based on the smeared crack model [6][8]. Consequently, this carefully considered model very effectively represents the dynamic behavior of systems with repeated arbitrary load paths. It should be noted, however, that stiffness reduction and deterioration in materials due to repeated loading are not considered. Thus, the stress path returns independently to the original value when strain relaxes back to the maximum experienced value. In the overall response of structure, however, due to the combination of path-dependent material models, the reaction value slightly decreases under cyclic loading when displacement returns to the maximum experienced value.

The material models inserted into the frame analysis are adjusted to ensure accuracy in spite of the degeneration of degrees of freedom and to be consistent with the conventional three-dimensional constitutive models of reinforced concrete [9]. The concrete model is assumed to have the following five characteristics:

- 1) Cracking criteria [6] depend on the loading path;

- 2) The elasto-plastic fracture model is used for compressive zone [6][8];
- 3) A tension stiffening model representing bond effect is used for the tensile zone [6][10];
- 4) Smooth transition between compression and tension is assumed [6][10];
- 5) A zoning method, in which RC members are divided into a bond-affected area and an unaffected-area, is introduced [11];

A tri-linear model is adopted for steel in tension considering the bond effect and the localization of plasticity including rupture [12][13].

In the current analysis, pull-out of reinforcing bars from the footings, spalling of cover concrete, and buckling of reinforcing bars in the highly inelastic range are not taken into account. These behaviors may contribute to increased maximum and residual deformation. However, their effects on overall deformation are known to be rather small in real-scale structures because ratios of cover thickness and bar diameter to cross-sectional area are relatively small [14]. Moreover, accurate spalling and buckling models have yet to be completed. Thus, in this study, it is assumed that the analysis will underestimate the response and residual displacement in cases where the highly inelastic range is reached. Further research will be necessary to establish constitutive models to deal with such situations. The deformation of shear-prone structures is expected to be smaller than structures not prone to shear because the shear stiffness is assumed to be very large. Geometrical nonlinearity is introduced to take into account the P-delta effect in this model.

## 2.2 Structure Modeling and Failure Criterion

In modeling RC railroad bridges, the assumption is made that they are simply comprised of piers and a slab. Thus, foundations such as footings and piles are not included in the model. Soil is considered indirectly when identifying the ground motion at each location. Beam/column elements defined by in-plane theory are used to represent the RC piers, and three-dimensional solid elastic elements represent the slabs under the assumption that, in the case of railroad viaducts, they suffer no damage during an earthquake. These modeling assumptions are adopted as a means to reduce analysis time and to achieve practical application of three-dimensional dynamic analysis based on material nonlinearity. The slabs and piers form a continuous system in these structures. This is an advantage when using this method of structural analysis because it is not necessary to model the support devices.

Looking at the boundary conditions for the model, the pier bases are fixed with respect to translation and rotation, and ground motion is introduced into fixed nodes as an acceleration history. Structural damping is not considered. Also, the phase difference of the ground motion at different points is not taken into account; the motion is treated as identical at each point. Looking into the significance of the phase difference will require a future study. The system modeled consists of two spans or three-span frames, and the ends of the slabs are modeled as having free boundary conditions. This means that the influence of adjacent viaducts is neglected.

This analytical method does not aim at making a judgement directly of failure; rather, calculations are continued until the defined final step. However, if the concrete compression strain reaches  $-0.01$  by the end of analysis, it is judged that crushing of the cover concrete has occurred and the computation is terminated. The reason for this is that concrete stress falls to almost zero when the strain is high, and analytical convergence and accuracy deteriorate. In real structures, this failure criterion may be close to the heavily damaged state of flexure beyond which the cover concrete spalls. For other cases of failure, analysis is performed indirectly through post-processing as follows.

The shear failure criterion of a rectangular section is defined as an ellipse representing the locus of shear capacity in the longitudinal and transverse

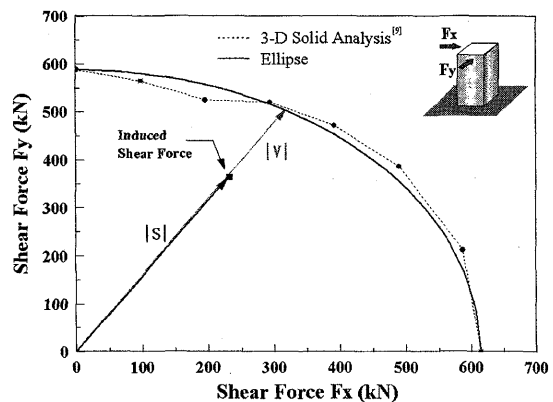


Fig.2 Shear Capacity of RC Column under Multi-directional External Forces [5][16]

directions [17]. These capacities are calculated using an empirical formula. The failure orientation of a structure can be computed by this method [5][16]. Based on the defined criteria, failure analysis is implemented after completing the simulation by comparing the induced shear force with the shear capacity at each time step. The sum of the squares of induced shear forces in the longitudinal and transverse direction ( $|S|$ ) is calculated. The safety evaluation is performed by comparing this value  $|S|$  against the shear capacity in the same of direction ( $|V|$ ), as shown in Fig.2 [5][16]. Note that the shear capacity depends on the axial force and the degree of flexural deformation at any time step.

The contribution of concrete to shear capacity in the longitudinal and transverse directions is calculated using the Niwa-Okamura Equation [18] including factor  $a/d$ , which is a revision of the Okamura-Higai Equation [19]. The Niwa-Okamura Equation is defined below in Eqs. (1) to (4). The contribution of stirrups to shear capacity is generally calculated based on Truss Theory, but here the effect of steel is neglected because the RC piers of interest have few stirrups and no reinforcement effect may be expected. This capacity evaluation method itself can be verified through the investigation with numerical simulation for many structures.

$$V_c = 0.20f_c^{1/3} (0.75 + 1.4d/a) b_w d \beta_p \beta_n \beta_d \quad (1)$$

$$\beta_p = (100p)^{1/3} \leq 1.5 \quad (2)$$

$$\begin{aligned} \beta_n &= 1 + M_0 / M_d \leq 2 \quad (N'_d \geq 0) \\ &= 1 + 2M_0 / M_d \geq 0 \quad (N'_d \leq 0) \end{aligned} \quad (3)$$

$$\beta_d = (1000/d)^{1/4} \leq 1.5 \quad (4)$$

where  $V_c$  is the contribution of concrete to shear capacity (N),  $f_c$  is concrete compressive strength (MPa),  $b_w$  is the width of the cross section (mm),  $d$  is the effective depth (mm),  $a$  is the shear span length (mm),  $p$  is the reinforcement ratio in the tension zone,  $M_d$  is a counter-flexural moment nullifying the stress induced by axial force on the tension fiber of the member,  $M_0$  is the design flexural moment, and  $N'_d$  is the design uni-axial compressive force (N).

In this method, the value  $p$  is automatically obtained in each time step based on the stress value of the reinforcing bars. Similarly, the effect of the induced axial force is also automatically considered as part of the induced bending moment at each time step. This is expressed as  $\beta_n$  in the empirical equation.

### **3. EFFECT OF MULTI-DIRECTIONAL GROUND MOTION**

#### **3.1 General**

In past research [7], it has been shown through numerical simulation that the response and residual displacement of a single RC pier model is high under multi-directional ground motion. It is also reported that the shear failure criterion for a rectangular section in a diagonal direction can be defined as an elliptical locus connecting the shear capacity in the longitudinal and transverse directions [17]. Consequently, it may be induced that structural response and capacity when the ground motion is multi-directional would be different from the two-dimensional behavior during horizontally uni-directional ground motion.

It is clear that little particular attention is paid to multi-directional ground motion in the present design method used in Japan. Rather, it is implicitly included in the safety factor. However, it is now the period of transition to performance-based design. Performance-based design — which can be regarded as the next generation of design system — requires evaluations of not only capacity but also residual displacement or performances after an earthquake. For this reason, there is a need to directly consider the effects of multi-directional ground motion. Three-dimensional analysis methods using degenerated frame elements or mindlin plate elements have been improving rapidly in recent times, and their practical accuracy has already been verified. Therefore, there is reason to conclude that a three-dimensional approach is now more rational than a two-dimensional one. Two-dimensional approach needs equivalent transformation to three-dimensional one in order to consider multi-directional effects [7][15].

In this study, three different ground motion input methods are considered: three-directional input (two horizontal directions & vertical direction), two-directional inputs (longitudinal horizontal direction & vertical direction and transverse horizontal direction & vertical direction). By comparing the results of applying different ground motions, the influence of each component on the seismic performance of RC frames in railroad viaducts is verified. Through analysis using only the two horizontal ground motions, the influence of the vertical component on the overall structural response is also examined.

### 3.2 Target Structure and Input Ground Motion

A summary of the target structure is given in Fig. 3. The ratios of shear and flexural capacity in the longitudinal and transverse directions are indicated in Table 1. The design values of material strength are used for these calculations. The compressive strength of the concrete  $f'_c$  is  $240 \text{ (kgf/cm}^2\text{)} = 23.5 \text{ (MPa)}$ , and the main reinforcing bar yield strength is  $f_y$  is  $3,500 \text{ (kgf/cm}^2\text{)} = 343 \text{ (MPa)}$ . The piers are named  $C_{a1}$  to  $C_{a8}$  for convenience, as illustrated in Fig. 3. The structure is judged as being low in seismic performance in the first stage evaluation, and heavily damaged due to shear cracking in reality.

Although identifying ground motion remains very difficult at present, it is desirable to select as reliable a motion as possible. Here, the ground motion at each location is identified from latitude and longitude using the method proposed by Annaka et al. [21]. The identified seismic waves for the site in the three directions are shown in Fig. 4.1 to Fig. 4.3. The component in the north-south direction is called the NS component, that in the east-west direction EW and that in the vertical direction UD in this paper. The acceleration time history of the seismic motion is input at 0.02 (s) intervals in the dynamic analysis. In order to reduce analysis time, only the main part of the identified seismic wave, between approximately 10 and 15 (s), is used, since it is this part that affects the structural response.

The NS component is aligned such that it corresponds with the transverse direction, and the EW component with the longitudinal direction. This is not exactly in accord with reality, since railroad lines do not always run east-west. However, it could be reasoned that there is no significant difference between the identified waves in the two horizontal directions, and the input direction of ground motion is then dealt with simply.

### 3.3 Analytical Results and Consideration

First, the analytical results for the EW component (longitudinal direction) and UD (vertical direction) are shown in Figs. 5-1 to 5-4. These indicate the induced shear force and shear capacity time histories of piers  $C_{a1}$ ,  $C_{a2}$ ,  $C_{a3}$ , and  $C_{a4}$ . The orientation of induced shear force and that of shear capacity always coincide. In this analysis with only one horizontal input, the EW component, the induced shear force is much less than the shear capacity for all piers. It is worth noting, incidentally, that results for piers  $C_{a5}$ ,  $C_{a6}$ ,  $C_{a7}$ , and  $C_{a8}$  are very similar to those for  $C_{a1}$  to  $C_{a4}$ , respectively. (Only the results for  $C_{a1}$  to  $C_{a4}$  are shown below.)

Next, the analytical results for the NS component (transverse direction) and UD (vertical direction) are shown in Figs. 6-1 to 6-4. As with Fig. 5, these indicate the induced shear force and shear capacity time histories, and once again the induced shear force and shear capacity orientations always coincide. This analysis of only the NS component, the induced shear force also falls short of the shear capacity for all piers. The difference between induced shear force and capacity for  $C_{a2}$ , however, is small at 6.60 (s).

Finally, the analytical results for two horizontal components and UD are shown in Figs. 7-1 to 7-4. In this case, conversely, the induced shear force of  $C_{a2}$  and  $C_{a4}$  rises beyond the shear capacity. This means that the mode of failure shifts from flexure to shear. This demonstrates that the effect of multi-directional ground motion should not be neglected.

Shear failure of  $C_{a2}$  and  $C_{a4}$  occurs almost simultaneously, with  $C_{a2}$  at 6.46 (s) and  $C_{a4}$  at 6.44 (s). The ratio of shear to flexural capacity for  $C_{a4}$  is the smallest, and the shear capacity of  $C_{a1}$  is the smallest. Nevertheless,  $C_{a2}$  suffers shear failure at almost the same time as  $C_{a4}$ . Details of the analytical result for multi-directional ground motion are discussed below.

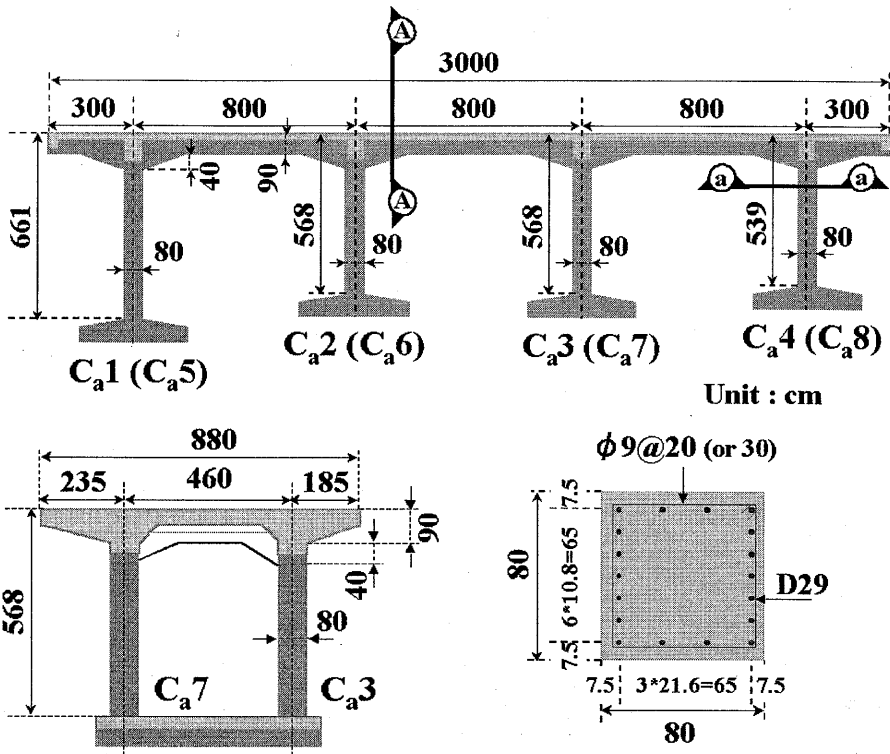


Fig.3 Target Structure

Table 1 Capacity Ratio of Shear and Flexure ( $V_u \cdot a / M_u$ )

	Longitudinal Direct.	Transverse Direct.
C <sub>a1</sub>	1.07	1.17
C <sub>a2</sub> , C <sub>a3</sub>	0.93	1.02
C <sub>a4</sub>	0.89	0.98

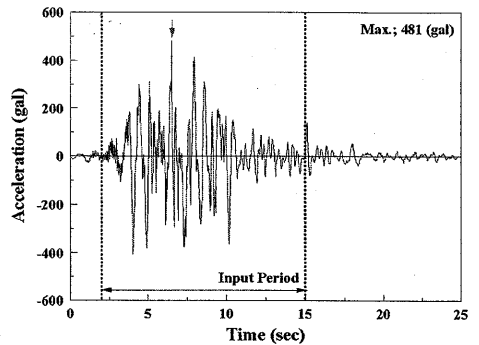


Fig.4.1 NS Component of Ground Motion

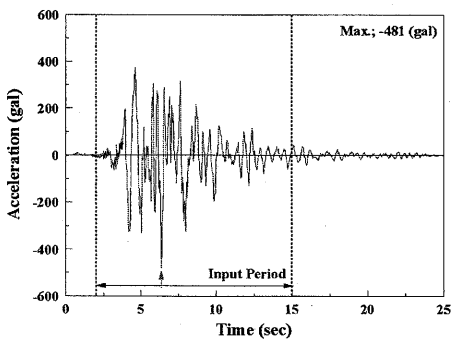


Fig.4.2 EW Component of Ground Motion

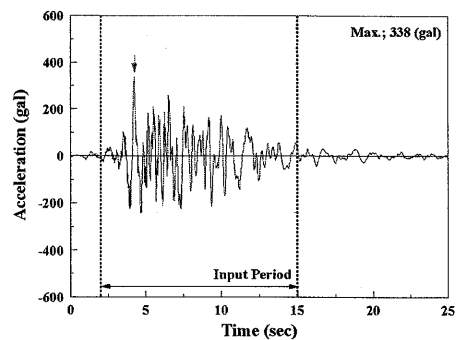
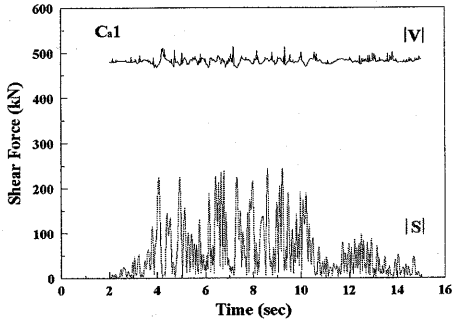
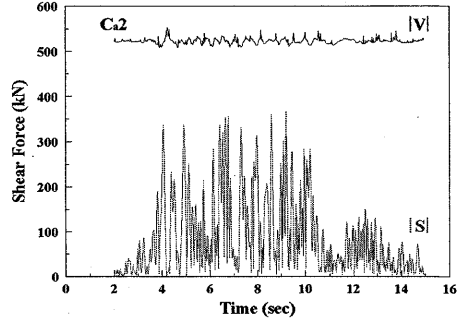


Fig.4.3 UD Component of Ground Motion



**Fig.5.1** Induced Shear Force and Shear Capacity Time Histories of C<sub>a1</sub> (EW&UD Components)



**Fig.5.2** Induced Shear Force and Shear Capacity Time Histories of C<sub>a2</sub> (EW&UD Components)

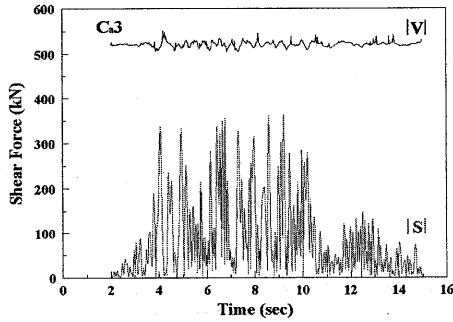


**Fig.5.3** Induced Shear Force and Shear Capacity Time Histories of C<sub>a3</sub> (EW&UD Components)

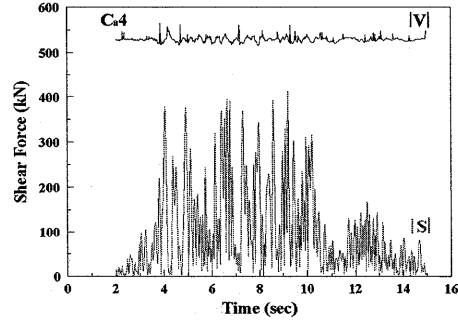


**Fig.5.4** Induced Shear Force and Shear Capacity Time Histories of C<sub>a4</sub> (EW&UD Components)

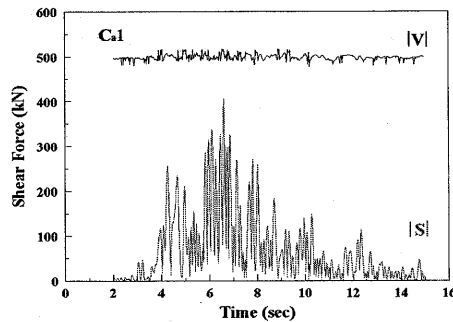


**Fig.6.1** Induced Shear Force and Shear Capacity Time Histories of C<sub>a1</sub> (NS&UD Components)

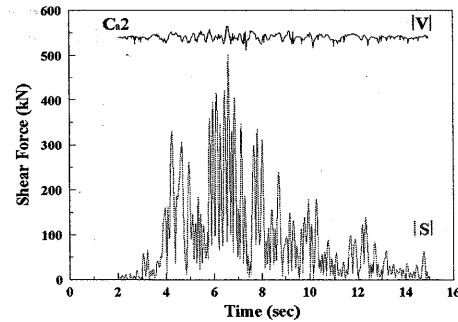


**Fig.6.2** Induced Shear Force and Shear Capacity Time Histories of C<sub>a2</sub> (NS&UD Components)

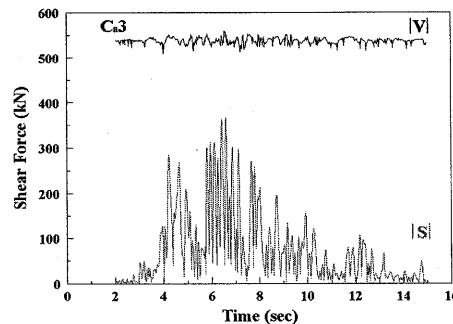


**Fig.6.3** Induced Shear Force and Shear Capacity Time Histories of C<sub>a3</sub> (NS&UD Components)

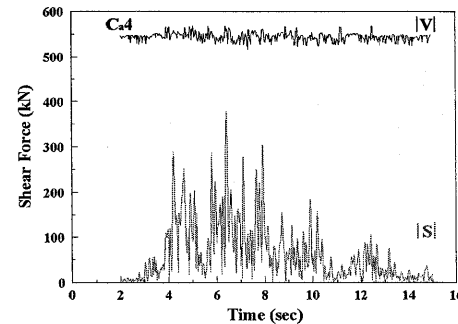


**Fig.6.4** Induced Shear Force and Shear Capacity Time Histories of C<sub>a4</sub> (NS&UD Components)

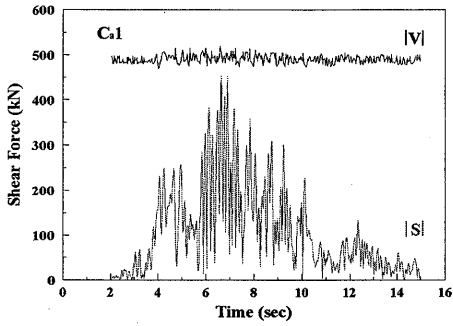


Fig. 7.1 Induced Shear Force and Shear Capacity Time Histories of  $C_{a1}$  (Three Components)

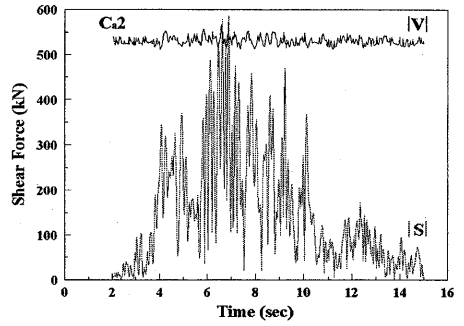


Fig. 7.2 Induced Shear Force and Shear Capacity Time Histories of  $C_{a2}$  (Three Components)

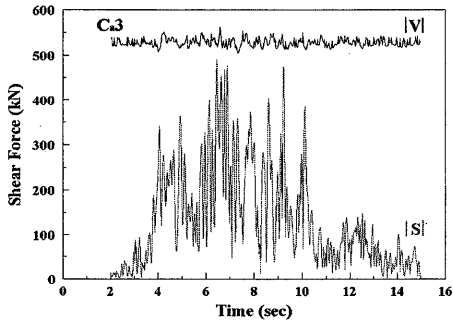


Fig. 7.3 Induced Shear Force and Shear Capacity Time Histories of  $C_{a3}$  (Three Components)

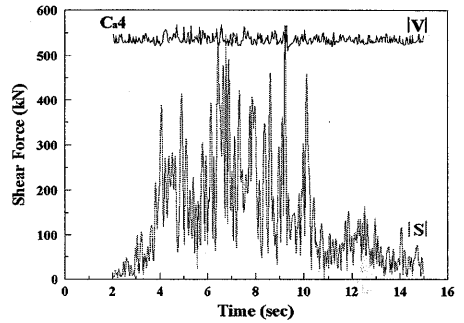


Fig. 7.4 Induced Shear Force and Shear Capacity Time Histories of  $C_{a4}$  (Three Components)

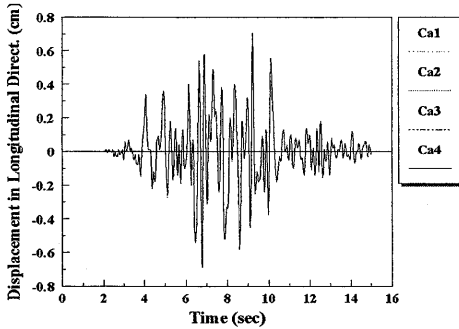


Fig. 8.1 Response Displ. in Longitudinal Direction

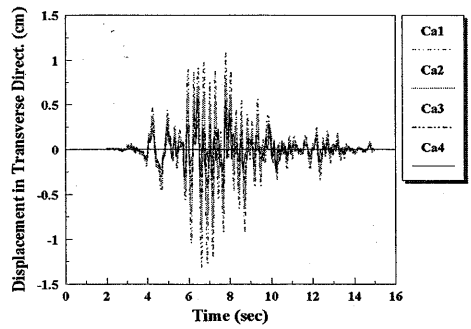


Fig. 8.2 Response Displ. in Transverse Direction

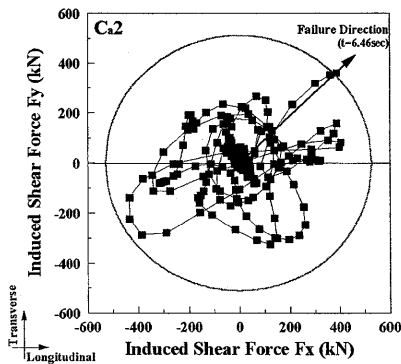


Fig. 9.1 Induced Shear Force and Failure Envelope ( $C_{a2}$ )

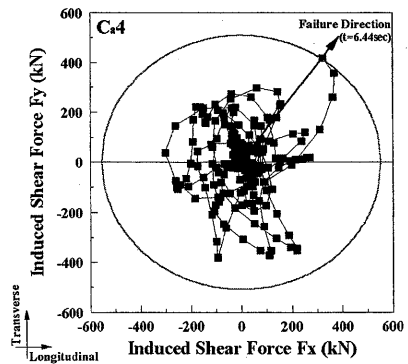


Fig. 9.2 Induced Shear Force and Failure Envelope ( $C_{a4}$ )

The response displacement time history for  $C_{a1}$  to  $C_{a4}$  in the longitudinal and transverse directions are illustrated in Figs. 8.1 and 8.2. In the longitudinal direction, three span frames stand end to end, and all piers ( $C_{a1}$  to  $C_{a4}$ ) respond uniformly (Fig. 8.1). In the transverse direction, as shown in Fig. 8.2, the response displacements of  $C_{a1}$  to  $C_{a4}$  differ. All piers respond directly to the torsional condition of the top slab. This derives from the unequal heights of the piers, and is determined by the stiffness of the tallest pier  $C_{a1}$  lying at the extremity and the shortest pier  $C_{a4}$ . Consequently, it can be expected that a relatively large load is induced on  $C_{a2}$  because the deformation of  $C_{a1}$  pulls  $C_{a2}$  and shear failure occurs very early. This tendency is developed in the analysis using seismic motion in the transverse and vertical directions. As this introduction of multidirectional ground motion demonstrates,  $C_{a2}$  and  $C_{a4}$  fail in shear almost simultaneously. The failure envelope and induced shear force for  $C_{a2}$  and  $C_{a4}$  at each time step are indicated in Figs. 9.1 and 9.2. These diagrams make it quite clear that the failure orientation of this structure is a line almost mid-way between the longitudinal and transverse directions.

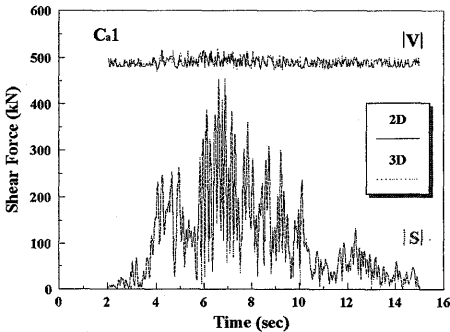


Fig.10.1 Induced Shear Force and Shear Capacity Time Histories ( $C_{a1}$ )

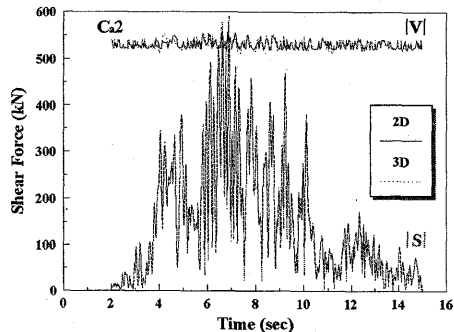


Fig.10.2 Induced Shear Force and Shear Capacity Time Histories ( $C_{a2}$ )

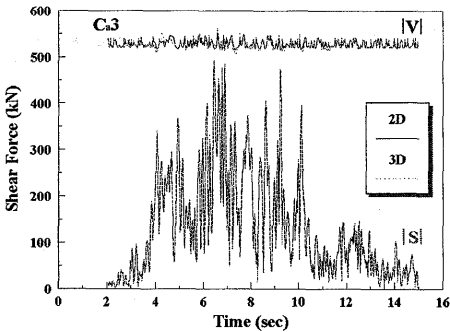


Fig.10.3 Induced Shear Force and Shear Capacity Time Histories ( $C_{a3}$ )

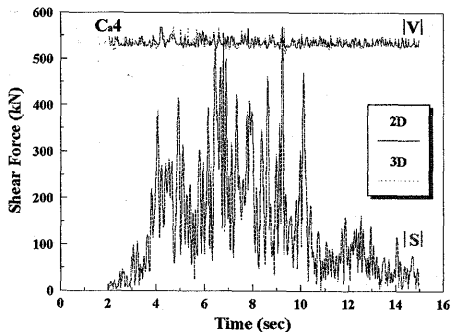


Fig.10.4 Induced Shear Force and Shear Capacity Time Histories ( $C_{a4}$ )

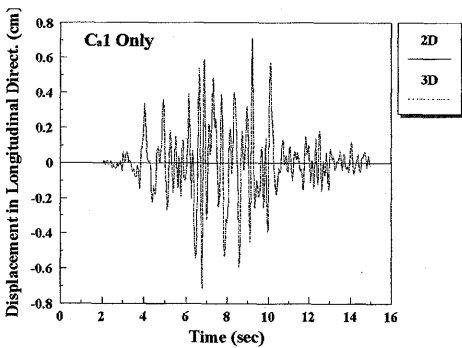


Fig.11.1 Response Displ. in Longitudinal Direction

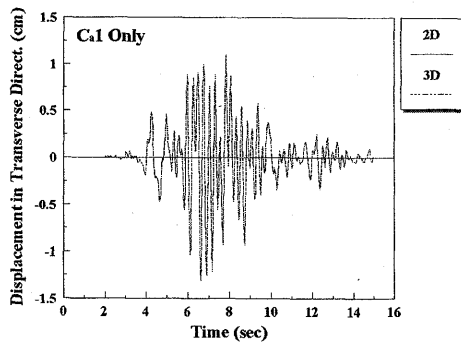


Fig.11.2 Response Displ. in Transverse Direction

This consideration of the results demonstrates clearly that the target structure, whose ratio of shear and flexural capacity is very close, requires three-dimensional dynamic analysis based on multi-directional ground motion as the second stage evaluation. Multi-directional ground motion causes a change in the failure mode. Moreover, the point of failure and the failure orientation are strongly influenced by the motion. These phenomena are not easily explained using two-dimensional analysis with one-dimensional horizontal ground motion. Structures susceptible to flexural failure when subjected to multi-directional ground motion may exhibit a larger response and residual displacement due to the effect of bending along two axes as compared with one horizontal motion. This effect is also difficult to take into account in a two-directional analysis.

In order to examine the influence of vertical motion on structural response, analysis with only the two horizontal components is also carried out. Comparing the results with two horizontal components with those obtained for all three components, the shear force demand and shear capacity time histories are shown in Figs. 10.1 to 10.4, and the response displacements in Figs. 11.1 to 11.2. Regarding the response displacement, although only  $C_a1$  is shown, the other piers exhibit the same tendency.

Figure 10 indicates that there is little difference between the two cases. The slight difference in shear capacity can be attributed to fluctuations in the axial force due to the presence of vertical motion. There is also little difference in the longitudinal and transverse response displacements in the two cases (Fig. 11). An analysis in which a single RC pier is modeled has indicated similar results [7]. Generally, it might be considered that the influence of vertical motion can be ignored where the ratio of compressive strength and axial stress imposed by the superstructure is small, as is often the case in the infrastructure.

#### **4. INFLUENCE OF MATERIAL STRENGTH VARIATIONS ON FAILURE CONDITION**

##### **4.1 Target Structure and Material Strength**

In the analysis described above, the design values are used for the material strengths. Namely, the compressive strength of concrete  $f'_c$  is  $240 \text{ (kgf/cm}^2\text{)} = 23.5 \text{ (MPa)}$  and the yield strength of the main reinforcing bars  $f_y$  is  $3500 \text{ (kgf/cm}^2\text{)} = 343 \text{ (MPa)}$ .

These values are selected since actual material properties identified by sampling or other methods are difficult to obtain. However, it is desirable to use actual data for material properties in order to obtain accurate results. For establishing the seismic evaluation method, it is expected that the accumulation of database on structures and material properties would be carried out, and that research environment would be improved by using the database efficiently.

The influence of material strength on the seismic performance of the overall structure should be investigated because assumed values of material strength are used. Generally, the design strength can be taken as a minimum value, and the actual value would be higher. Here, by raising the compressive strength of concrete and the yield strength of reinforcement uniformly by 25 (%) and 29 (%), respectively, a comparative analysis of the variation in material strength is conducted. Thus, in this case,  $f'_c$  is  $300 \text{ (kgf/cm}^2\text{)} = 29.4 \text{ (MPa)}$  and  $f_y$  is  $4,500 \text{ (kgf/cm}^2\text{)} = 441 \text{ (MPa)}$ . While these increases in material strength are determined empirically, they can be considered valid if compared with the literature [1][22]. The tensile strength of concrete  $f_t$  is not made altered, and remains at  $22 \text{ (kgf/cm}^2\text{)} = 2.2 \text{ (MPa)}$ .

A summary of the structure is shown in Fig. 12. The piers are named  $C_b1$  to  $C_b8$  for convenience. The ratio of capacity values obtained using the design values and the incremented values of material strength are indicated in Table 2. Increasing the material strength as defined above leads to a decrease in seismic performance of the structure as a whole [22]. The shear capacity increases in line with the changes in material strength, but flexural capacity increases beyond the rising rate of the shear capacity. This is because the flexural capacity increases in approximate proportion to the yield strength of the steel, while the shear capacity rises in proportion to the cubic root of concrete compressive strength, as indicated by Eq. (1).

The failure mode of the structure can be expected to shift from flexure to shear when the material strengths are increased by 25 (%) for concrete and 29 (%) for steel. Thus, the target structure may be suitable to conduct the comparative analysis on material strength variation. Dynamic analysis for varying material strengths and a consideration of seismic performance are discussed in the next section.

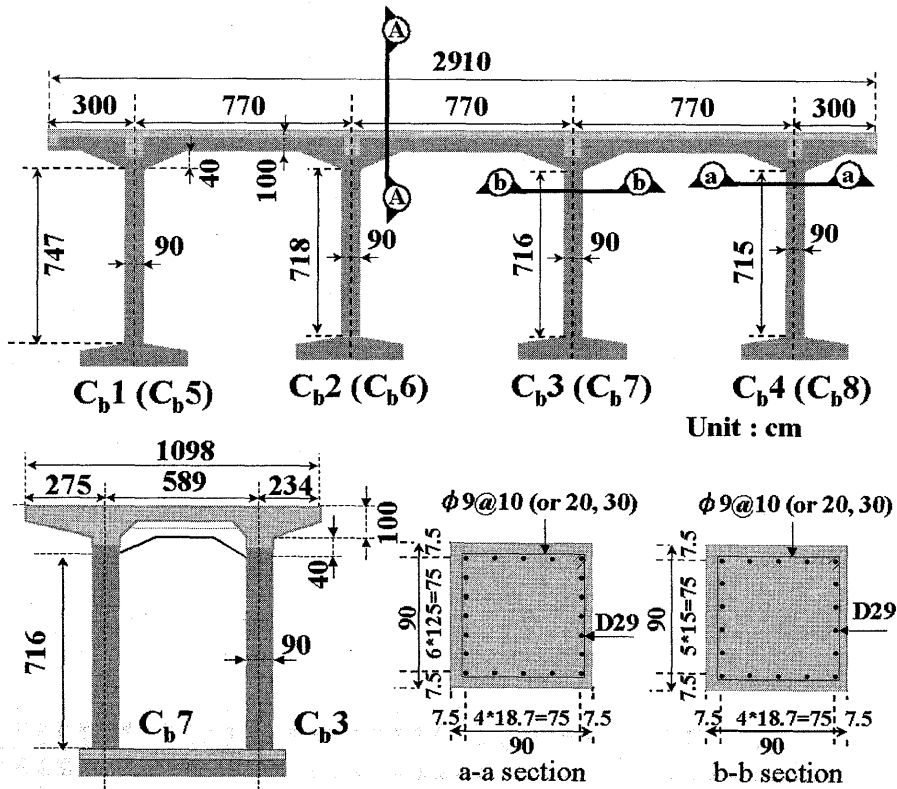


Fig.12 Target Structure

Table2 Capacity Ratio of Shear and Flexure ( $V_u \cdot a / M_u$ )

	Longitudinal Direct.	Transverse Direct.
C <sub>b1</sub>	1.37/0.94	1.35/0.93
C <sub>b2</sub>	1.47/1.01	1.43/1.02
C <sub>b3</sub>	1.35/0.93	1.34/0.93
C <sub>b4</sub>	1.33/0.91	1.31/0.91

Left figure; design strength is used.

Right figure; increased strength is used.

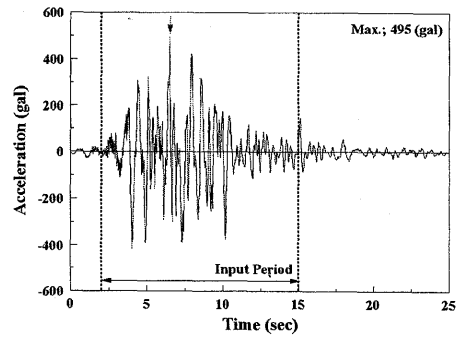


Fig.13.1 NS Component of Ground Motion

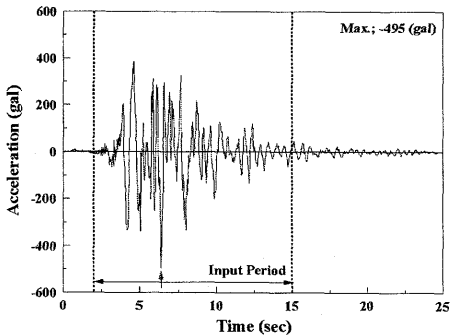


Fig.13.2 EW Component of Ground Motion

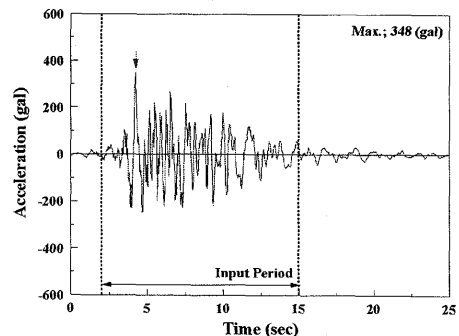
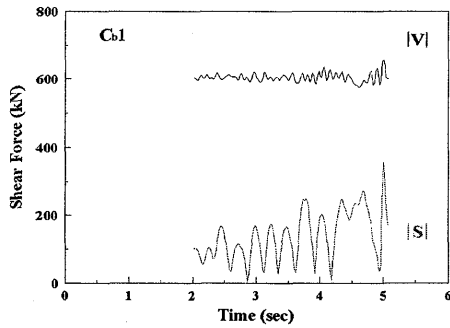
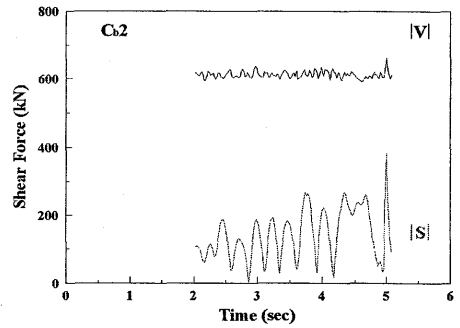


Fig.13.3 UD Component of Ground Motion



**Fig. 14.1** Induced Shear Force and Shear Capacity Time Histories of  $C_{b1}$  (Design Strength)



**Fig. 14.2** Induced Shear Force and Shear Capacity Time Histories of  $C_{b2}$  (Design Strength)

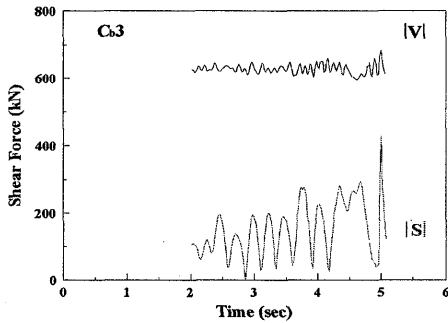


**Fig. 14.3** Induced Shear Force and Shear Capacity Time Histories of  $C_{b3}$  (Design Strength)

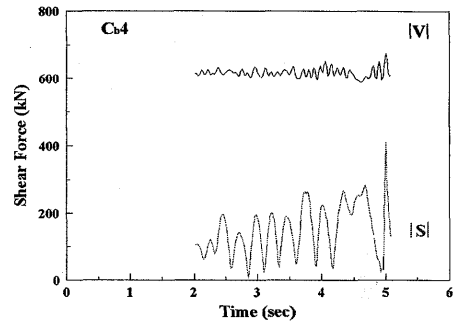


**Fig. 14.4** Induced Shear Force and Shear Capacity Time Histories of  $C_{b4}$  (Design Strength)

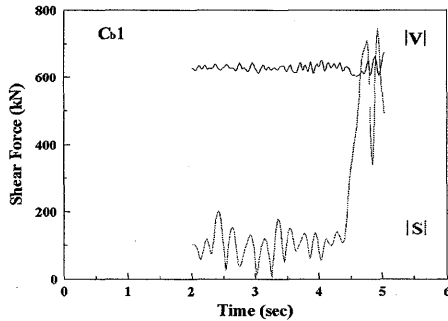


**Fig. 15.1** Induced Shear Force and Shear Capacity Time Histories of  $C_{b1}$  (Increased Strengths)

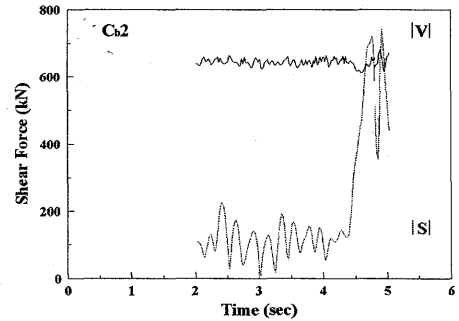


**Fig. 15.2** Induced Shear Force and Shear Capacity Time Histories of  $C_{b2}$  (Increased Strengths)

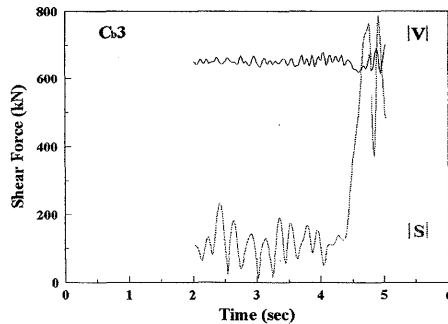


**Fig. 15.3** Induced Shear Force and Shear Capacity Time Histories of  $C_{b3}$  (Increased Strengths)

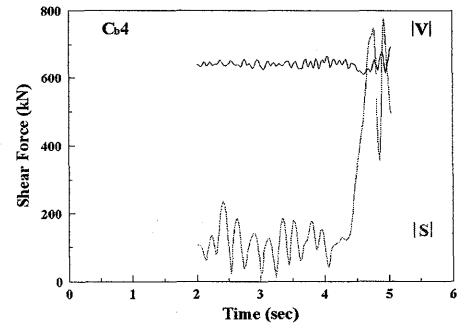


**Fig. 15.4** Induced Shear Force and Shear Capacity Time Histories of  $C_{b4}$  (Increased Strengths)

## 4.2 Results of Comparative Analysis and Consideration

The seismic waveforms shown in Figs. 13.1 to 13.3 are identified as the ground motion at the surface for this comparative analysis. Three components, NS, EW, and UD, are input to the target structure.

As illustrated in Figs. 14.1 to 14.4, induced shear force clearly falls below shear capacity when the analysis adopts the design values of material strength. In this case, however, the computation terminates due to a judgement that the concrete has failed under compressive strain at time point 5.10 (s). This is assumed to be flexural failure. On the other hand, when the increased values of material strength are used, the induced shear force rises above shear capacity for all piers (see Figs. 15.1 to 15.4). Flexure-prone piers become shear-prone ones as the values of material strength rise. This result agrees with the prediction based on reduction in capacity ratio mentioned in the previous section.

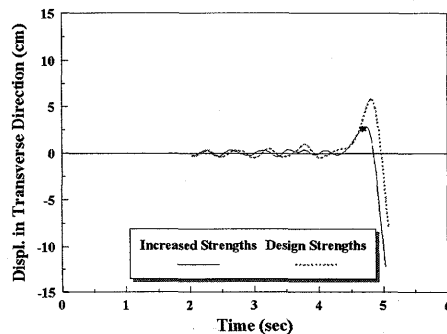
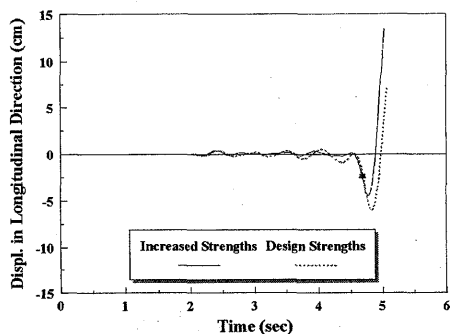


Fig.16.1 Response Displ. in Longitudinal Direction

Fig.16.2 Response Displ. in Transverse Direction

Time histories of response displacement in the longitudinal and transverse directions and focusing on the strength variation are illustrated in Figs. 16.1 and 16.2. The response displacement of each pier in the two orthogonal directions is nearly equivalent up to termination. Since all piers behave similarly, pier C<sub>1</sub> only is picked up for illustration in Fig. 16. It is clear that the natural period of the structure changes significantly as a consequence of the increases in material strength. While the structure modeled with design values yields, and both response and residual displacements are large, the displacements are smaller when the increased values of material strength are used because the yield strength and stiffness increase until shear failure. Yielding occurs just before termination in the case of the structure with the increased strength values, and considerable plastic deformation is introduced. However, these changes are excluded from the consideration here because the structure has already reached shear failure by this point. The main point, though, is that this method of dynamic analysis reinforces the finding that seismic performance decreases when the actual concrete compressive strength and steel yield strength are uniformly higher than the design values.

These results indicate that, when carrying out damage analysis, special attention should be paid to values of material strength. The strength of steel might have already reached enough industrially reliable level except at joints and splices at the time of construction. In fact, based on sampling tests, it can be said that the actual steel yield strength is likely to be approximately 1.25 times the design value. This value should be used if the actual strength is unknown [1]. Generally, it is difficult to determine the strength of concrete because there is a large variation. To overcome this problem, dynamic analysis of many structures needs to be carried out, and the average of the sampled values taken. In the meantime,  $\alpha$  (= about 1.0 – 1.2) times the design strength can be adopted for the time being. There is also a need for this numerical method to be thoroughly verified through a macroscopic analysis comparing the analytical results and observed damage.

## 5. CONCLUSIONS

A three-dimensional nonlinear dynamic method of for evaluating the seismic damage to RC frames in railroad viaducts is proposed as part of an overall damage analysis method. Evaluation depends on the latest technology, which is presently incomplete but still reaches a practical engineering level, backed up by engineering

judgements. In this case, the target structures are RC frames in railroad viaducts only, but the proposal should be applicable to any structure consisting of beams and columns.

To prepare for application of this method of dynamic analysis to many different types of structure, comparative studies on the influence of multi-directional ground motion and on the effects of variations in material strength values have been performed. This analytically demonstrated that a three-dimensional approach is essential to the consideration of multi-directional ground motion, and further that material strength values play a crucial role.

The next step will be to carry out three-dimensional dynamic nonlinear analysis for many cases in order to implement a damage analysis of structures. This is necessary because the proposed method includes three types of uncertainty:

- 1) Uncertainty in the technology for identifying ground motion
- 2) Uncertainty in the reliability of structural analysis tools used for seismic performance evaluation
- 3) Uncertainty in the actual values of material properties in target structures

Some of the uncertainties have already arrived at the approximately engineering practical level, or verification data has been accumulated. However, it is vitally important to accumulate some sample data and make appropriate judgments if this technology is to be put into use while our knowledge includes some areas of incompleteness. In other words, this statistical work will enable us to improve our methods of identifying ground motion, our design equations used to determine capacity, our structural analysis tools, and our estimates of material strength.

The final aim is to fully clarify the factors that influence the seismic performance of whole structures. Before reaching that goal, there are many problems to be overcome, such as the response mechanism of the whole structure including the foundations and piles and the influence of adjacent viaducts. It is the responsibility of the Japan Society of Civil Engineers to rationally explain the response of all structures to earthquakes, to learn lessons from events, and to apply them to the next generation of structures.

## Acknowledgements

The writing of this paper was made possible largely through gratis offers of software applications, one for identifying ground motion and the other for carrying out structural analysis. The former was kindly given by Mr. Mitsuo HARADA of TEPCO, and the latter by Prof. Koichi MAEKAWA of the University of Tokyo. The authors wish to express the gratitude to the members of the research committee (under the Concrete Committee of the JSCE) that carried out "Damage Analysis of Hanshin-Awaji Great Earthquake" (Chairperson: Prof. Hidetaka UMEHARA, Nagoya Institute of Technology).

## References

- [1] Editing Committee of the Damage Investigation Committee of the Great Hanshin-Awaji Earthquake: Investigative Report on the Great Hanshin-Awaji Earthquake – Damage to Infrastructure, Bridge Structure, December 1996 (in Japanese)
- [2] Okamura, H.: Japanese Seismic Design Codes Prior to the Hyogoken-Nanbu Earthquake, *Cement and Concrete Composites*, Vol. 19 (3), pp.185-192, 1997
- [3] JSCE: Damage Analysis of the Great Hanshin-Awaji Earthquake and the Design Equation for Ductility Ratio [Special Investigative Research Committee on the Great Hanshin-Awaji Earthquake, WG Report], *Concrete Engineering Series 12*, JSCE, July 1996 (in Japanese)
- [4] Okamura, H., Maekawa, K., and Kim, I.H.: Seismic Performance Diagnosis and Evaluation Method for Concrete Structures, *Proceedings of 30<sup>th</sup> Memorial Symposium of the Foundation of Nishinippon Institute of Technology*, pp.29-36, 1998 (in Japanese)
- [5] Kim, I., Okamura, H., and Maekawa, K.: Method for Checking Seismic Performance of Concrete Structures and its Effectiveness, *Journal of Structural Engineering*, Vol.44A, pp.165-170, 1998
- [6] Okamura, H. and Maekawa, K.: Nonlinear Analysis and Constitutive Models of Reinforced Concrete, *Gihodo-Shuppan*, May 1991
- [7] Tsuchiya, S., Fukuura, N., and Maekawa, K.: Dynamic Response of RC Piers Subjected to Multi-Directional Forces Using 3-Dimensional FEM Analysis based on Fiber Model, *Proceedings of the*

- Repetition Deterioration Phenomena in the Plastic Range Symposium*, pp.359-368, JCI, Aug. 1998 (in Japanese)
- [8] Maekawa, K. and Okamura, H.: The Deformational Behavior and Constitutive Equation of Concrete Using the Elasto-Plastic Fracture Model, *Journal of the Faculty of Engineering, the University of Tokyo (B)*, Vol.37, No.2, pp.253-328, 1983
  - [9] Hauke, B. and Maekawa, K.: Three-Dimensional Modelling of Reinforced Concrete with Multi-Directional Cracking, *Journal of Materials, Concrete Structures and Pavements*, No.634/V-45, pp.349-368, JSCE, November 1999
  - [10] Shima, H., Chou, L., and Okamura, H.: Micro and Macro Model for Bond Behavior in Reinforced Concrete, *Journal of the Faculty of Engineering, University of Tokyo (B)*, Vol.39, No.2, 1987
  - [11] An, X., Maekawa, K., and Okamura, H.: Numerical Simulation of Size Effect in Shear Strength of RC Beams, *Journal of Materials, Concrete Structures and Pavements*, JSCE, No.564/V-35, pp.297-316, May, 1997
  - [12] Fukuura, N. and Maekawa, K.: Computational Model of Reinforcing Bar under Reversed Cyclic Loading for RC Nonlinear Analysis, *Journal of Materials, Concrete Structures and Pavements*, No.564/V-35, pp.291-295, JSCE, May 1997 (in Japanese)
  - [13] Salem, H. and Maekawa, K.: Spatially Averaged Tensile Mechanics for Cracked Concrete and Reinforcement under Highly Inelastic Range, *Journal of Materials, Concrete Structures and Pavements*, JSCE, No.613/V-42, pp.277-293, February 1999
  - [14] The Metropolitan Expressway Public Corporation, Incorporated Foundation of the Metropolitan Expressway Technical Center: Investigation on Bridge Highways of the Metropolitan Expressway (1995) — *Report of Concrete Piers Subcommittee*, February 1996 (in Japanese)
  - [15] Tsuchiya et al.: Multi-Directional Flexure Behavior and Nonlinear Analysis of RC Columns Subjected to Eccentric Axial Forces, *Concrete Library of JSCE*, No.37, pp.1-15, June 2001
  - [16] Okamura, H., Maekawa, K., and Kim, I.: Next-Generation Design Method of Concrete Structures, *Concrete under severe conditions 2*, Vol.1, pp.3-16, 1998
  - [17] Yoshimura, M.: Failure Envelope of RC Columns in Two-Way Shear, *Summaries of Technical Papers of Annual Meeting*, AIJ, 1996
  - [18] Niwa, J., Yamada, K., Yokozawa, K., and Okamura, H.: Reevaluation of the Equation for Shear Strength of RC Beams without Web Reinforcement, *Concrete Library of JSCE*, No.9, pp.65-84, 1987
  - [19] Okamura, H. and Higai, T.: Proposed Design Equation for Shear Strength of Reinforced Concrete Beams without Web Reinforcement, *Proceedings of JSCE*, No.300, pp.131-141, August 1980
  - [20] JSCE: Standard Specification for Design and Construction of Concrete Structures [Design], 1996 (in Japanese)
  - [21] Annaka, T.: Reference I - Investigation on Definition of Ground Motion & Load, Guideline of Structural Performance Verification for LNG Underground Tank, *Concrete Library 98*, pp.39-56, 1999 (in Japanese)
  - [22] Abe, S., Fujino, Y. and Abe, M.: An Analysis of Damage to Hanshin Elevated Expressway during 1995 Hyogoken Nambu Earthquake, *Proceedings of JSCE*, No.612/I-46, pp.181-199, January 1999. (in Japanese)